# Transient aerodynamic pressures and forces on trackside and overhead structures due to passing trains. Part 1 Model scale experiments Part 2 Standards applications

Baker, Christopher; Jordan, S.; Gilbert, T.; Quinn, A.; Sterling, M.; Johnson, T.; Lane, J.

*DOI:*
10.1177/0954409712464859



*Document Version*
Early version, also known as pre-print

*Citation for published version (Harvard):*
Baker, C, Jordan, S, Gilbert, T, Quinn, A, Sterling, M, Johnson, T & Lane, J 2014, 'Transient aerodynamic pressures and forces on trackside and overhead structures due to passing trains. Part 1 Model scale experiments Part 2 Standards applications', *Proceedings of the Institution of Mechanical Engineers Part F Journal of Rail and Rapid Transit*, vol. 228, no. 4, pp. 36-69. https://doi.org/10.1177/0954409712464859

# Transient aerodynamic pressures and forces on trackside and overhead structures due to passing trains. Part 2 Standards applications

C Baker*, S Jordan, T Gilbert, A Quinn, M Sterling

Birmingham Centre for Railway Research and Education, University of Birmingham, Birmingham B15 2TT

T Johnson, J Lane

RSSB, Block 2, Angel Square, 1 Torrens Street, London, EC1V 1NY

*Corresponding author – c.j.baker@bham.ac.uk, +44 (0)121 414 5067

**Abstract**

This paper is the second part of a two part paper that describes the results of an experimental investigation to measure the load transients on railway structures due to passing trains. Part 1 described the model scale experiments that were carried out and the results that were obtained. This paper further analyses the results in terms of the development of new formulations for standards that would be relevant to trackside structure geometries commonly found in the UK. Specifically it compares the experimental results with the formulations of the existing standards, and shows that they are very conservative for the UK situation. This is largely due to the fact that the standard formulations were derived from experiments and calculations based on European train sizes and track geometries, whereas the trains in the UK are somewhat smaller. Two methods of correcting for different train size were evaluated and both were shown to bring the loads predicted from the standards closer to the experimental results. Formulae were then derived from the experimental data for the aerodynamic loading on a variety of typical trackside structures that may be useful in future standards revisions.

**Keywords** – train aerodynamics, aerodynamic pressures, bridges, hoardings, canopies, platforms

## 1. Introduction

Part 1 of this paper describes a series of aerodynamic experiments carried out using the moving model TRAIN Rig to measure the transient aerodynamic pressure loads on trackside and overhead structures. The rationale for this tests, fully described in Part 1, was to measure the transient loading on a wider range of trackside and overhead structure geometries than was possible in earlier full scale experiments, for a number of different train types, so that an in depth understanding of the flow phenomena could be achieved, and also, more practically, to provide information on the loading of structures of relevance to GB operating conditions, to supplement the current code which was developed for continental loading gauges ([1], [2] and to provide material for a UK National Annex to these standards. The tests were carried out using models of three different types of train (a streamlined Class 390 Pendolino leading car, a two car blunt fronted Class 158 multiple unit, and a Class 66 freight locomotive) for a number of different trackside and overhead structures (hoardings, overbridges, canopies and trestle platforms). Part 1 describes the nature of these experiments, and outlines the results that were obtained. The results were compared, as far as possible, with the results from other full scale and model scale experiments, and a broad level of consistency and reliability was demonstrated. From these results the following main conclusions could be drawn concerning the general nature of these pressure transients.

a) The use of the TRAIN rig methodology has been shown to be a robust way of obtaining aerodynamic loading on a wide variety of trackside structures in an efficient manner, with the results show good run-to-run repeatability.

b) The nose pressure coefficient distribution caused by passing trains is of the expected type, with a positive pressure peak followed by a negative pressure peak. In general, the peaks are not symmetrical i.e. the positive and negative peaks do not have the same magnitudes.

c) In general the surface pressure coefficients generated by the Class 66 freight locomotive are greater than those generated by the Class 158 multiple unit, which are themselves greater than those generated by the Class 390 Pendolino.

d) A comparison of the current results with a range of earlier measurements and calculations at both model scale and full scale show a reasonable agreement, although the nature of many of the earlier results makes a precise comparison difficult.

This paper uses the experimental results to consider a number of issues relevant to the codification of aerodynamic pressure transient loading on structures, Section 2 sets out the current codification procedure used in [1] and [2]. Section 3 then presents a comparison of the experimental loading data with the uncorrected code values, and the code values corrected for the difference in continental and GB loading gauges through two different methods. Section 4 then casts the experimental data into a format that is directly comparable with the codification method and this is then used in section 5 to develop a series of relationships for structural loading in UK conditions that will form the basis of a proposal for a National annex to the code. Finally some conclusions are drawn in section 6.

**2. The current codification procedure**

One aspect of the current work was to use the experimental data to suggest revisions to current codification procedures to cover GB specific conditions. Now the current procedure outlined in

[2] for describing the train induced aerodynamic loads on structures makes the basic (design) assumption that the pressure wave is of the form shown below for the forces on vertical structures next to the track (Figure 1), horizontal structures above the track (Figure 2) and canopy structures (Figure 3).

In each case, the pressure pulse is assumed to consist of a constant positive pressure that extends for a distance of 5m ahead of the train for vertical structures (Figure 1) or from the front of the train nose for horizontal structures (Figure 2), with a constant negative pressure of 5m length immediately following. There would thus appear to be some discrepancy between the assumed position of the pressure transient relative to the train for vertical and horizontal structures, although in reality this will not be of importance, since the load on the structure is required, without reference to train position. The magnitudes of the positive and negative pressures are assumed to be the same. From the results presented in part 1, this can be seen to be only a very rough approximation of reality, with the measured pressure distributions showing rather sharper positive and negative peaks (i.e. less than 5m in length), and whilst for some of the results the magnitudes of the positive and negative peaks are similar, this is far from the general situation. This point having been made, in each case, the loadings on the structures are calculated from the following expressions.

For vertical structures next to the track (hoardings)

$$p_{1k} = 0.5\rho V^2 k_1 C_{p1} \qquad C_{p1} = \frac{2.5}{(Y+0.25)^2} + 0.02 \qquad (1)$$

$\rho$ is the density of air and $V$ is the train speed, $C_{p1}$ is a pressure coefficient and $Y$ is defined in Figure 1. $k_1$ takes on a value of 1.0 for freight trains, 0.85 for conventional passenger trains and 0.6 for streamlined high speed trains.

For horizontal structures above the track (overbridges):

$$p_{2k} = 0.5\rho V^2 k_2 C_{p2} \qquad C_{p2} = \frac{2.0}{(h-3.10)^2} + 0.015 \qquad (2)$$

and $h$ is defined in Figure 2. $k_2$ takes the same values as $k_1$.

For canopy like structures.

$$p_{3k} = 0.5\rho V^2 k_3 C_{p3} \qquad C_{p3} = \frac{1.5}{(Y+0.25)^2} + 0.015 \qquad k_3 = \frac{7.5-h}{3.7} \qquad (3)$$

where $h$ is again defined in Figure 3. $k_3$ is dependent on the value of h and there is thus assumed to be no dependence upon different types of train in this case. The dependence upon $h$ is only applicable within the range of h used in the measurements i.e.4.0m <$h$<6.0m

In attempting to understand the genesis of the above method, the experiments of [3] were analysed. The nature of the experimental data that was obtained was not altogether clear. It would seem that different methods were used to find the spatially averaged loads on horizontal and vertical structures. For the former, a simple averaging of the lateral pressure distribution was carried out. For the vertical stuctures however a “moment averaging” was carried out about the base of the structure i.e. the moment of the measured pressures around the base were calculated and then divided by the height of the structure to give a pseudo-force value. From the report it is however not clear how the 5m long peak values were obtained. It appears likely

that for vertical structures next to the track, the experimental pressure data was averaged over a 5m length across the maximum and minimum peaks, to take account of the effective spacing between fence supports, but for horizontal structures, the maximum peak value was taken to apply over the entire 5m length, and that these led to the values in the code. Also it should be noted that for over track structures such as overbridges, the peak values of pressure measured at the centre of the track were assumed to act over up to a 10m length either side of the track centre. Now the results of Part 1 for 10m span overbridges show a very considerable falling off in pressure magnitude away from the centreline and this is also likely to be the case for longer span overbridges, potentially making this a very conservative assumption.

Now whilst the above procedure is criticisable on a number of grounds, in what follows the experimental results have been analysed in a manner that is consistent with this methodology. For all the results, the positive and negative pressure peaks were calculated as the average values over 5m lengths before and after the main zero crossing point. For horizontal structures, either the average value of such peaks in the lateral direction have been calculated (canopies), or the distribution in this direction considered (trestle platform and overbridges). For vertical structures (hoardings) the “moment averaged” value has been calculated over the structure height, (although in reality this differs little from the arithmentically averaged value in almost all cases).

**3. Direct comparison of results with code values.**

In this section, we compare the experimental results outlined earlier with the provisions of the code for the three types of structure for which the code makes allowance – vertical structures parallel to the track (hoardings), horizontal structures above the track (overbridges) and

horizontal structures to the side of the track (canopies). Before making this comparison, it must be noted that the code values were determined for the larger continental loading gauge, and thus for a structure at a fixed distance from the side of the track or above the rail, the effective separation between train and structure is thus higher for GB trains than for continental trains, and some allowance needs to be made for this.

Two such methods were used in this study. In the first, an increment has been added to the distance from the track to the structure when using the equations set out in section 2 – effectively the difference between the continental G1 gauge and the GB W6A gauge, giving a lateral increment of 0.24m (the difference between the maximum half width of the above gauges) and a vertical increment of 0.36m (the difference between the maximum heights), allowing corrections to be made for structures at both the side of and above the track. This has been applied to the hoarding, bridge and canopy results. The second approach used the methodology developed in [4] They demonstrated that the pressure coefficients on a stationary train passed by a moving train scaled with the inverse square of the separation distance between the vehicles. This methodology was applied to the hoarding results, with the predicted pressure coefficients from equation (1) being multiplied by $((Y-W_{G1})/(Y-W_{W6A}))^2$, where $Y$ is the distance from the track centreline to the hoarding, $W_{G1}$ is the semi-width of the continental G1 gauge and $W_{W6A}$ is the semi-width of the GB W6A gauge. This correction should be regarded as only a first approximation, since the actual vehicles may well be smaller than the relevant gauge.

Figures 4 a, b and c show such a comparison between the hoarding experimental pressure coefficient data and the code provisions, with no corrections and the distance and pressure coefficient corrections respectively. Note that the code values, shown as continuous lines for

positive values and broken lines for negative values, do not apply for a distance from the track centreline of less than 2.3m. The symmetric nature of the code values for the positive and negative pressure peaks can be seen. The conservative nature of the uncorrected code provisions is clear. In general the experimental results are in broad agreement with the code values for both types of correction, and it is not altogether obvious which is to be preferred.

Figure 5 shows the comparison with the experimental pressure coefficient results for 10m wide overbridges and the code values, with no correction and using the distance increment correction to the code values. Note that in accordance with the methodology used in deriving the code values, the actual maximum experimental peak values are used, rather than the 5m average values. The experimental values are the centre line values ($y$=0), and make no allowance for the fall off in pressure away from the centre line described in part 1 of this paper. The uncorrected code values are again clearly conservative. For the Class 390 and Class 158 the corrected code values are still conservative, although for the Class 66, the experimental negative peaks are significantly higher than the corrected code values. The reasons for this rather poor agreement may well lie in the type of analysis used in the evaluation of the experimental data from [3] for the CEN code, that effectively assumed a symmetry between positive and negative peaks. However the precise nature of this analysis is not clear from [3] in terms of how this concept of symmetry is applied.

Figure 6 shows a comparison between the experimental results for the 4.7m high (above the track) open canopy pressure coefficient distribution and the equivalent code values, again with no correction and with the distance correction applied to the code values. In this case, both the horizontal and vertical gauge increments have been applied. Experimental results were only available for the freight train case, and the code makes no provision for trains of different types.

There is again reasonable agreement for the corrected values, although they are again non-conservative for the negative peak values.

Thus it can be seen that there is a broad equivalence between the current results and the corrected code values, although the lack of transparency in the calculating of code values from experimental results, and the necessity to impose corrections for loading gauge differences, makes it difficult to say any more than this. Nonetheless it does appear that the corrected Class 66 experimental values can at times exceed those indicated in the code.

## 4. Analysis of experimental data

In this section an analysis of the experimental data of part of this paper is presented in a form that is consistent with that used in [2] i.e. with the maximum values calculated over a 5m distance before and after the major zero crossing between the positive and negative peaks. For the sake of consistency this procedure is carried out for all structures, although, as pointed out above, it seems that for overbridges the code is based on peak rather than average values.

### 4.1 Hoardings experimental data

Figure 7 shows the experimental pressure coefficient data for trackside mounted and platform mounted hoardings. These values have been obtained by the “moment average” method as outlined above. As before the Class 66 peaks have the largest magnitudes and the Class 390 the smallest. The positive pressure peak drops off with hoarding distance from the track / platform edge in a consistent way. However the behaviour of the negative peak is somewhat different, particularly for the trackside hoardings, where the variation with distance from the track

is complex. There is significant positive / negative peak asymmetry here, reflecting the asymmetry in the pressure distributions.

### 4.2 Overbridge experimental data

Figure 8 shows the maximum and minimum peak pressure coefficients for overbridges. For the 10m wide overbridges of different heights, there can be seen to be a reduction in coefficient values as the height is increased, with the Class 66 pressure magnitudes being the largest and the Class 390 the smallest. For the 4.5m high overbridge of different widths, there can be seen to be little change to the coefficients for widths greater than 3m, but the 1.5m width values are less. However one must question whether the use of a 5m averaging length is appropriate for overbridges with a width in the train direction of less than this. For bridges less than 10m in width, an averaging length of half the bridge width might be most appropriate, which would result in rather greater loads. The results are broadly symmetric, with similar values for the positive and negative peaks, although there is a tendency for the latter to fall off less as the height increases.

### 4.3 Canopy experimental data

Figures 9 a to c shows the average canopy forces for the different trains, plotted in terms of both canopy height and back wall distance. Only the smallest and largest back wall distances and heights are shown for clarity, the data for the other tests carried out falling between these. An examination of the figures shows clearly there is a decrease in the maximum peaks with height as seems reasonable, but such an effect is less apparent for the negative peaks. In general, the closer the backwall, the higher the canopy loadings.

### 4.4 Trestle platform results

Figure 10 shows the maximum and minimum peak pressure coefficients analysed in the same way as above for the trestle platform results. The results are broadly as expected, with a decrease in coefficient from the platform edge, and the Class 66 coefficients being the highest and the Class 390 the smallest. The results again show an asymmetry, with the negative peaks being larger than the positive peaks.

## 5 Development of new codification format

### 5.1 Outline

In this section we will consider how the experimental results can be put into a suitable format for supplementing the existing information in [2]. In particular we look to obtain curves of the following form used in the code.

For vertical structures next to the track (hoardings)

$$p_{1k} = 0.5\rho V^2 k C_{p1} \qquad C_{p1} = f_1(Y or\ Y') \tag{4}$$

where *Y* is the distance of the hoarding from the track centreline and *Y'* is the distance from the platform edge.

For horizontal structures above the track (overbridges)

$$p_{2k} = 0.5\rho V^2 k C_{p2} \qquad C_{p2} = f_2(h, W) \tag{5}$$

where *h* is the overbridge height above the track and *W* is the width of the overbridge in the along track (*x*) direction.

For canopies with back walls

$$p_{3k} = 0.5\rho V^2 k C_{p3} \qquad C_{p3} = f_3(h, Y) \tag{6}$$

where *h* is the height of the canopy above the track and *Y* is the distance of the backwall from the track centreline.

For trestle platforms, we consider curves for local loading of the form

$$p_{4k} = 0.5\rho v^2 k C_{p4} \qquad C_{p4} = f_4(y') \tag{7}$$

where *y'* is the distance from the edge of the platform.

Note that the factor that describes the effect of train type *k* will be taken to be the same in each case in order to eliminate the effect of train type. In addition for the overbridge case, it might be useful to parameterise the variation of load with distance across the track, although this is not taken into account for the existing codification process in [1] and [2].

In section 5.2, we firstly consider the determination of the factor *k* that describes the effect of different train types. In sections 5.3, 5.4, 5.5 and 5.6, we then consider the case of hoardings, overbridges, canopies and trestle platforms, respectively, and develop the appropriate form of the functions $C_{p1}$ to $C_{p4}$.

### 5.2 The effect of train type

To determine the effect of train type, for each of the train / structure configurations described in part 1, four ratios were found - the ratios of the peak positive and negative pressure coefficients for the Class 390 and Class 158 trains, to the equivalent values for the Class 66 train. These ratios were then used, giving each of the configurations equal weight, to find the average ratios for the Class 390 peaks to those for the Class 66 peaks, and the same ratio for the Class 158 peaks to the Class 66 peaks. The tabulated results are shown in Table 1. Note that this weighting of the different configurations is purely arbitrary, but the results are not particularly sensitive to the weighting used. These ratios, (i.e. *k* values), have values of 0.43 for the Class 390 to Class 66 loads, and 0.53 for the Class 158 to Class 66 loads (and 1.0 of course for the Class 66). Note that these are significantly less than would be expected from [2] (0.65 for streamlined trains and 0.80 for ordinary passenger trains), but reflect the experimental results that were obtained. It may well be that this difference arises because the locomotives that were used in the freight train experiments of [3], on which the results of [1] and [2] were based, SNCF BB7200 and BB9200, have frontal shapes that, whilst blunt, are a little more rounded than those of the Class 66. Also note the large spread of the results from the different configurations shown in table 1.

### 5.3 Hoardings

Figure 11 shows the hoarding experimental peak coefficients ($C_{pe}$) divided by the average k values for each train type. An envelope curve is also shown for the trackside and platform hoardings that encompasses the data in a conservative way. Note that the curve envelopes are symmetrical i.e. the lower value is simply the negative upper value. Such an approach

preserves the format of [2] but clearly involves significant conservatism. These curves are given by

$$C_{p1} = \pm \frac{6.0}{(Y+1.75)^2} \quad (8)$$

for the trackside mounted hoardings and

$$C_{p1} = \pm \frac{3.8}{(Y'+2.5)^2} \quad (9)$$

for the platform mounted hoardings.

**5.4 Overbridges**

We note firstly from Figure 8, that changes in overbridge width do not cause significant changes in loading, and thus the pressure coefficient in equation (5) will be taken to be a function of overbridge height only. Again the experimental pressure coefficient data was scaled with the appropriate *k* factors for each train type and upper and lower envelope curves derived. The results are shown in Figure 12 below.

The upper and lower envelope curves are given by the following form

$$C_{p2} = \pm \frac{6}{(h-1)^2} \quad (10)$$

Again the conservatism forced by the symmetry assumption can be seen. Although no specifically allowed form for lateral pressure variation was included in the formulations for the codification values, it is also possible to fit envelope curves to the lateral variation of pressure

coefficient with loading for the overbridges that were tested. Such a method results (Figure 13) in the following envelope curve.

$$C_{p2}(y) = C_{p2}(0)(1 - 0.03y^2) \quad (11)$$

It should however be noted at this point that these results apply to a bridge across a single track only. For two track running it will not be appropriate to allow for the lateral variation in the same way, as it is possible that trains may exist on both tracks at the same time, although, at the cost of a little complication, the lateral variation could be applied to the structure over both tracks on the outer side of the tracks, with a constant load value in the central portion.

**5.5 Canopies**

The loads on canopies with back walls are clearly a function of the height of the canopy and the back wall distance. To find the variation with back wall distance, the ratios were formed of the loads at each back wall distance from the nearest track to that at a distance of 2.7m from the nearest track. The results are shown in Figure 14 below. Each point on this Figure is an average of the ratio for four points – one for each canopy height for a particular train type and back wall distance.

The envelope curve is given by

$$r = 1 - 0.1(Y - 3.45)^2 \quad (12)$$

where *Y* is the distance from the track centre line. The experimental pressure coefficients were then divided by the appropriate values of *k* and *r* and the results are shown in Figure 15 below. An upper and a lower envelope line is also shown and is given by

$$\frac{C_{p3}}{r} = \pm \frac{6}{(h-0.1)^2} \quad (13)$$

which leads to

$$C_{p3} = \pm \frac{6}{(h-0.1)^2}(1 - 0.1(Y - 3.45)^2) \quad (14)$$

### 5.6 Trestle platform

Figure 16 shows the trestle platform experimental results divided by the appropriate value of *k* to remove the effect of train type, together with upper and lower envelope curves. These are given by the following expression.

$$C_{p4} = \frac{3}{(y'+2.2)^2} \quad (15)$$

## 6. Concluding remarks

There are a number of basic assumptions made in the codification process used in [2] that are worthy of comment at this point.

a) The first is that the positive and negative pressure peaks can appropriately be averaged over a 5m distance. This is potentially a non-conservative assumption in situations where it may be necessary to consider a shorter distance (e.g. narrow overbridges), as the absolute peak values can be much higher than the 5m average values. Also, such a procedure is certainly not appropriate for a structure of less than 5m width, (such as many pedestrian overbridges). It might therefore be appropriate to consider whether or not a shorter averaging length might be more appropriate for some structures and some trains.

b) Secondly the codification method contains an implicit assumption of symmetry between the positive and negative peaks, although the precise nature of this assumption is unclear i.e. whether the absolute maximum or absolute minimum value is chosen as the defining case. The results presented here show that this is rarely the case, with the positive peak being generally larger in magnitude than the negative peak, and this assumption leads to major conservatism in the derivation of design curves – a pressure coefficient envelope that comes close to, say, the positive peaks, may significantly overestimate the negative peaks, and vice versa. It may be worth considering whether the benefits of relaxing this assumption outweigh the increased code complexity that would result.

c) For horizontal structures above the track, such as overbridges, the assumption made in the code that the peak track centre line pressure can be applied over a 20m span has been shown to be very conservative, both from the current experiments which show a significant decrease in pressures away from the track centreline, and from a comparison with the full scale measurements made on an overbridge (Part 1). For a bridge over a single track, it would seem appropriate to make some allowance for this through the use of a length reduction factor in the code, although for two tracks, with the possibility of a train on both tracks beneath the bridge at the same time, such an allowance is probably not appropriate.

d) The code implicitly assumes static loading throughout. Now whilst this is entirely appropriate in most cases, for some lightweight or flexible structures other information is needed to enable, say, fatigue calculations to be carried out. Such calculations would not only require relative short term loadings, but would also require some information on the frequencies associated with the pressure transient events. Much information of this type could be extracted from the current experimental data.

Also, it is clear from reading the report of [3] on which [2] is based, that much of the codified data was based on the use of theoretical panel method CFD calculations from the early 1990s. These were essentially unverified at the time, and in the light of current developments in CFD their adequacy cannot necessarily be assumed. These results either need to be independently verified or replaced by more reliable data. There is a case that could be made for an extensive series of tests using the TRAIN Rig methodology to measure the loads on structures caused by continental gauge trains, in order to replace some of the less reliable data in the current code.

Thus, in conclusion it can be seen that the outputs from the project have highlighted a number of areas where further work could offer benefits to the railway industry. These are as follows.

- There is a need to investigate whether the degree of conservatism in the various assumptions, and in differences between the existing pressure curves in [1] and [2] and the experimental results, make any practical or economic difference in the design of typical railway structures.
- A robust 'gauge' correction method can be developed and verified based on the experimental results and some checks for the actual distance between real trains and lineside structures rather than the distance from the train 'gauge'. This method could be included within the UK National Annex to [1] and [2].
- There is a need to identify appropriate fatigue load spectra (magnitude and frequency) for fatigue sensitive structures.

## References

[1] BSI, Eurocode 1 Actions on structures – Part 2 Traffic loads on bridges BS EN 1991-2; 2003

[2] BSI, Railway applications — Aerodynamics — Part 4: Requirements and test procedures for aerodynamics on open track, BS EN 14067-4:2005+A1:2009

[3] ERRI, Loading due to dynamic pressure and suction from railway traffic. Effect of the slipstreams of passing trains on structures adjacent to the track. ERRI D189/RP1, 1994

[4] Johnson T, Dalley S, 1/25 scale moving model tests for the TRANSAERO Project. In "TRANSAERO- A European Initiative on Transient Aerodynamics for Railway System Optimisation", pp 123-135, Springer-Verlag Berlin, 2002, ISBN 3-540-433136-3, 2002

## Acknowledgements

The experimental programme was undertaken in connection with the RSSB funded research project T750 'Review of Euronorm design requirements for trackside and overhead structures subjected to transient aerodynamic loads', which was sponsored by the railway industry 'Aerodynamics GB Working Group'.

## Notation

$C_{pi}$ Code pressure coefficient (i=1 to 4)

$h$ Distance from top of rail to overbridge / canopy

$k$ Parameter that specifies the effect of train type

| | |
|---|---|
| $k_1$ | *k* parameter in equation 1 |
| $k_2$ | *k* parameter in equation 2 |
| $k_3$ | *k* parameter in equation 3 |
| $p_{ik}$ | Peak pressures used in code |
| *r* | Ratio defined in equation 12 |
| *V* | Train / model velocity |
| *W* | Width of overbridge in *x* direction |
| $W_{G1}$ | Semi-width of G1 loading gauge |
| $W_{W6A}$ | Semi-width of W6A loading gauge |
| *x* | Distance along the track |
| *y* | Lateral distance from centre of track |
| *y'* | Lateral distance from edge of platform |
| *Y* | Lateral distance of vertical structures from centre of track |
| *Y'* | Lateral distance of vertical structures from platform edge |
| *z* | Vertical distance from the track |

$z'$ Vertical distance from top of platform

$\rho$ Density of air

**Captions for figures**

**Figure 1** Vertical structure next to the track in [2] (hoarding)

**Figure 2** Horizontal structure above the track in [2] (overbridges)

**Figure 3** Horizontal structure adjacent to the track in [2] (canopies)

**Figure 4** Comparison of experimental pressure coefficient results with code values for 2m high trackside hoardings (a – no correction; b - distance increment correction; c – pressure coefficient correction, after [4] - applied to the pressure coefficient values from [2] and given in equation 1). Note [2] only valid for distances from track centre >2.3m)

**Figure 5** Comparison of experimental pressure coefficient results with corrected code values for 10m wide overbridges (a- no correction; b – distance increment correction)

**Figure 6** Comparison of experimental pressure coefficient results with corrected code values for 4.7m high canopy (a- no correction; b – distance increment correction)

**Figure 7** Maximum pressure coefficients for trackside and platform mounted hoardings (a – trackside mounted hoardings, b – platform mounted hoardings)

**Figure 8** Maximum pressure coefficients for overbridges (a – 10m wide overbridges of different heights, b – 4.5m high overbridges of different widths)

**Figure 9** Maximum pressure coefficients for canopies (numbers in legend indicate back wall distance from nearest rail)

**Figure 10** Maximum pressure coefficient distribution for trestle platform

**Figure 11** Maximum pressure coefficients for hoardings scaled with *k* factors to allow for the effect of different train types. (Vertical axis shows pressure coefficient / *k*; a – trackside hoardings; b – platform hoardings, solid and dotted lines show envelopes to data)

**Figure 12** Maximum pressure coefficients for overbridges scaled with *k* factors to allow for the effect of different train types. (solid and dotted lines show envelopes to data)

**Figure 13** Lateral variation pressure coefficient ratios for the overbridge results, scaled with centre line values

**Figure 14.** Ratio of canopy loads to load with a backwall distance 2.7m from nearest track (3.45m from track centreline) (solid and dotted lines show envelopes to data)

**Figure 15** Canopy experimental pressures divided by *k* and *r* to correct for train type and back wall distance (solid and dotted lines show envelopes to data)

**Figure 16** Experimental pressure coefficients for trestle platform divided by *k* value (solid and dotted lines show envelopes to data **)**

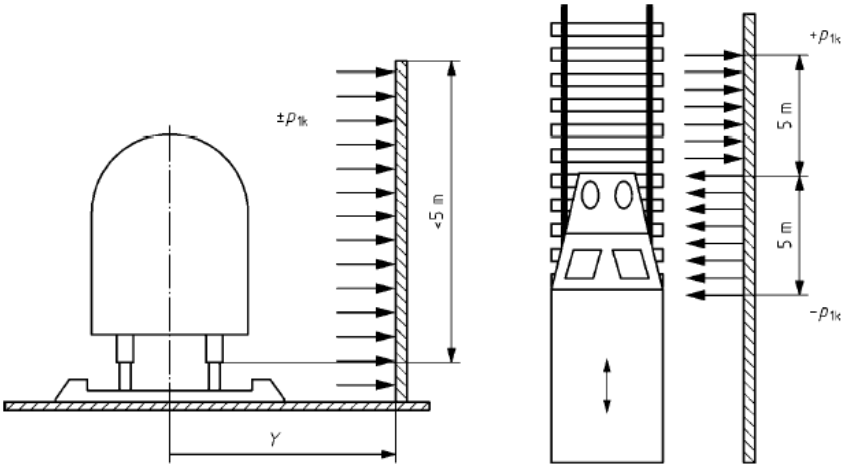


**Figure 1** Vertical structure next to the track in [2](hoarding)

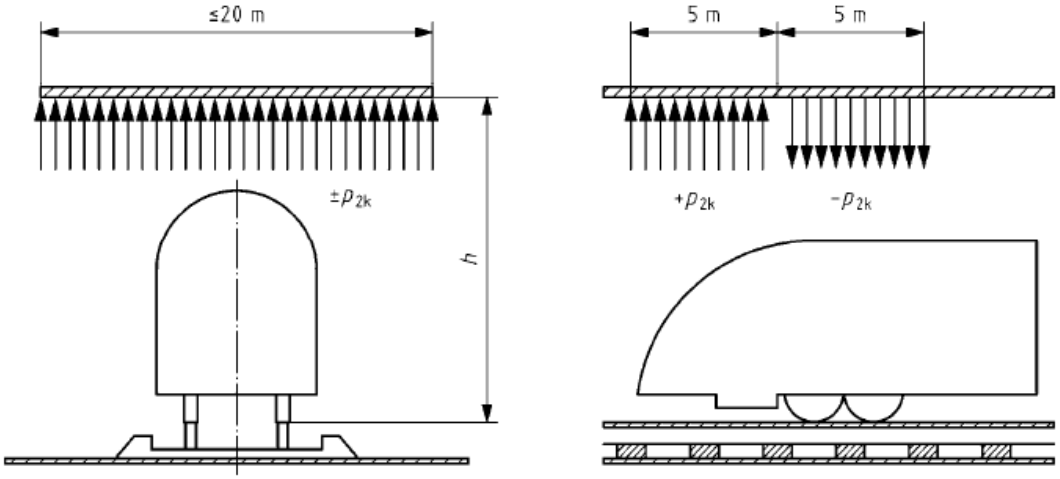


**Figure 2** Horizontal structure above the track in [2] (overbridges)

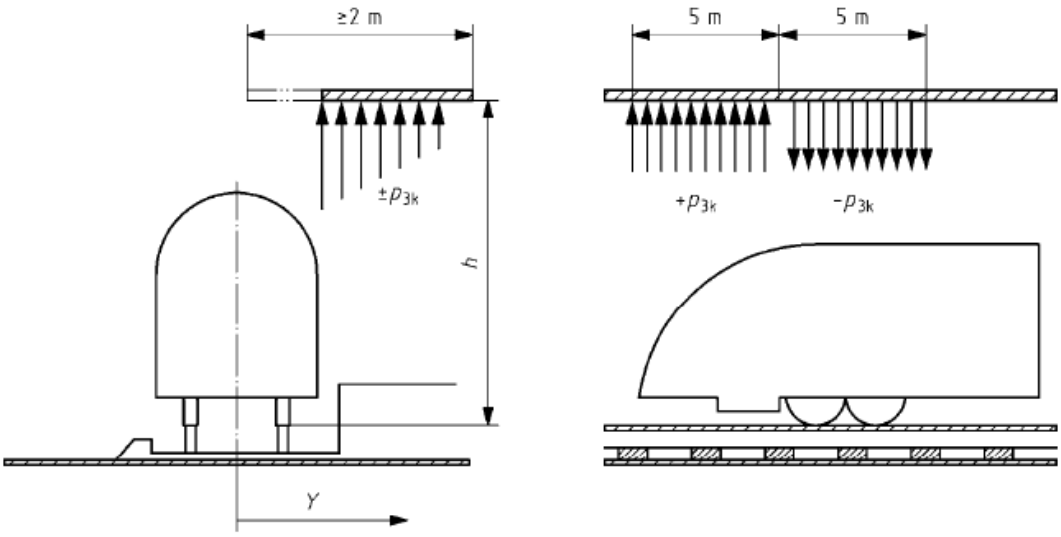


**Figure 3** Horizontal structure adjacent to the track in [2] (canopies)

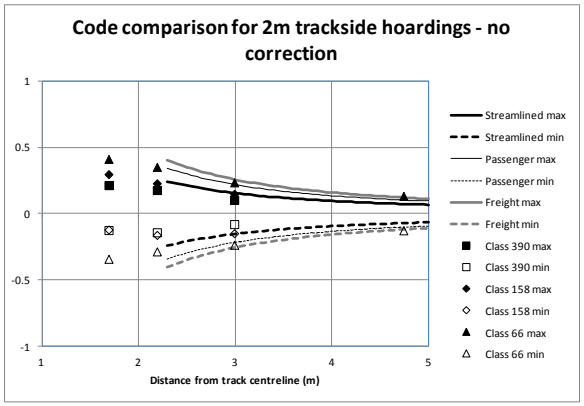


(a)

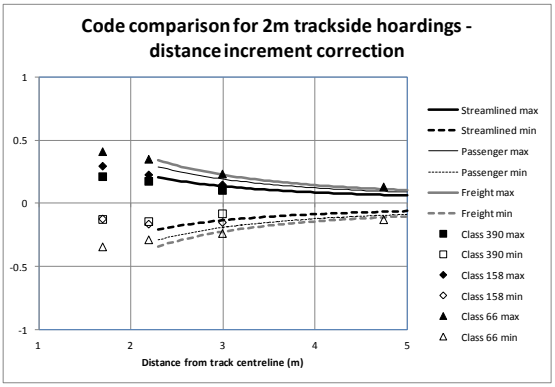


(b)

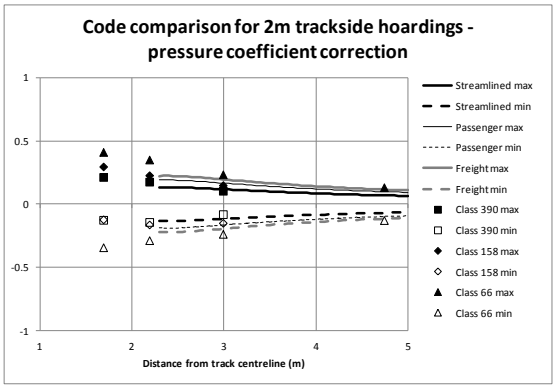


(c)

**Figure 4** Comparison of experimental pressure coefficient results with code values for 2m high trackside hoardings (a – no correction; b - distance increment correction; c – pressure coefficient correction, after [4] - applied to the pressure coefficient values from [2] and given in equation 1). Note [2] only valid for distances from track centre >2.3m)

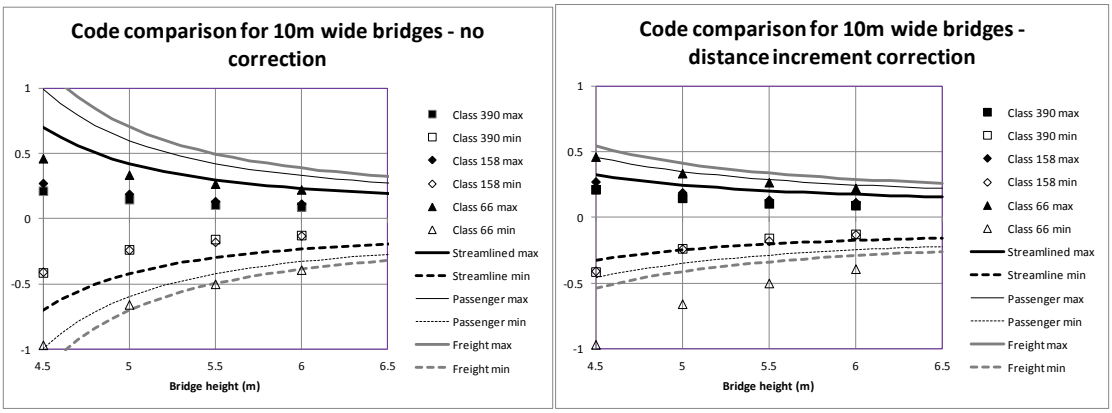


(a) (b)

**Figure 5** Comparison of experimental pressure coefficient results with corrected code values for 10m wide overbridges (a- no correction; b – distance increment correction)

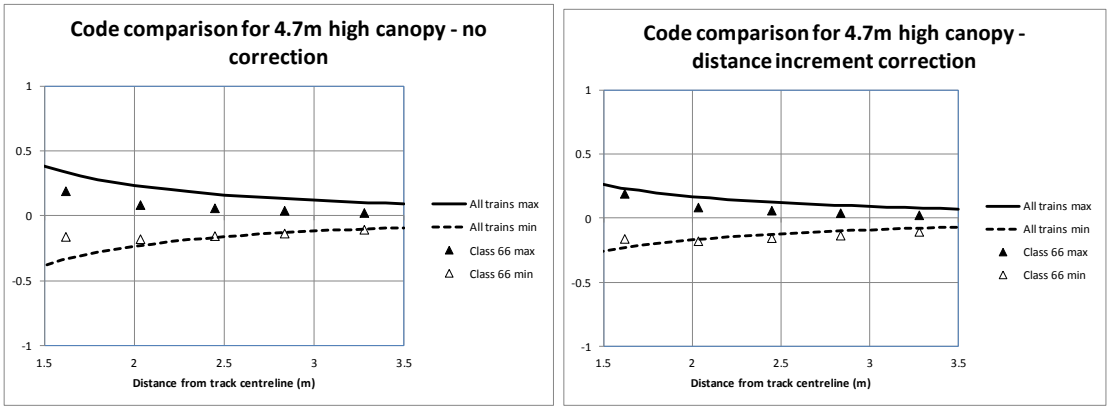


Figure 6 Comparison of experimental pressure coefficient results with corrected code values for 4.7m high canopy (a- no correction; b – distance increment correction)

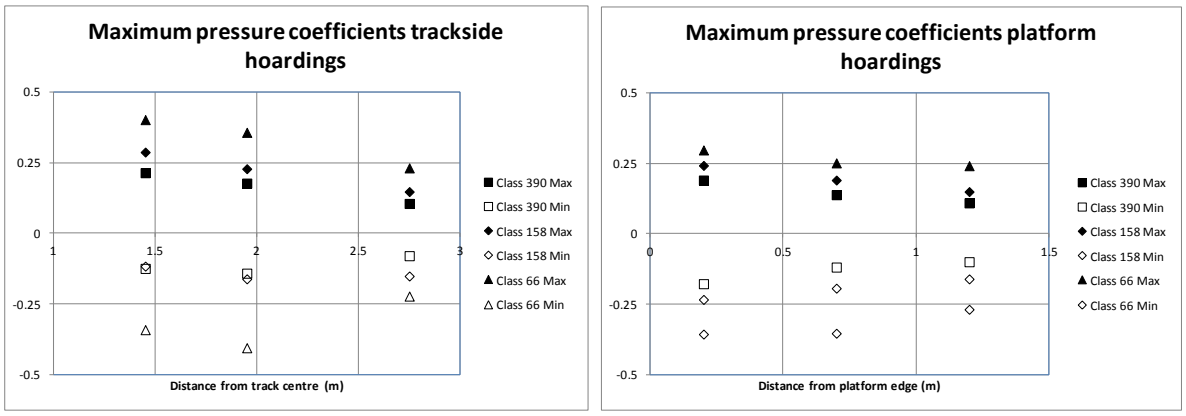


(a) (b)

**Figure 7** Maximum pressure coefficients for trackside and platform mounted hoardings (a – trackside mounted hoardings, b – platform mounted hoardings)

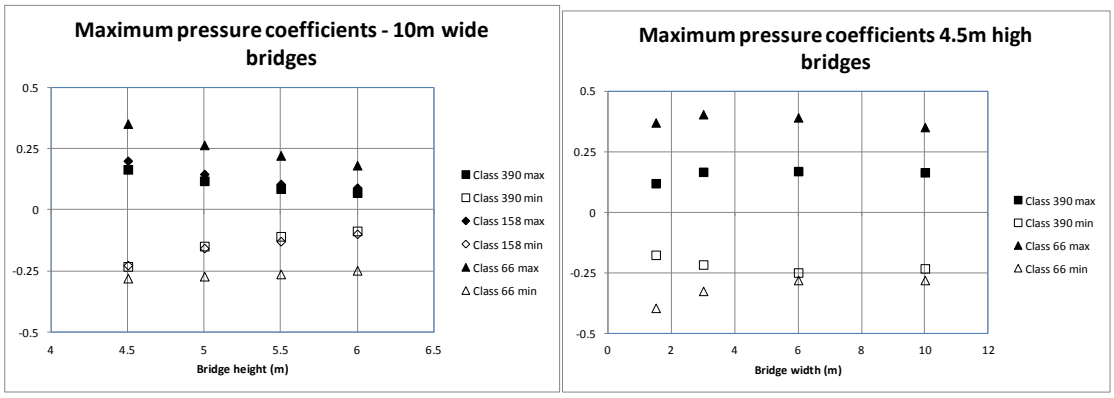


(a) (b)

**Figure 8** Maximum pressure coefficients for overbridges (a – 10m wide overbridges of different heights, b – 4.5m high overbridges of different widths)

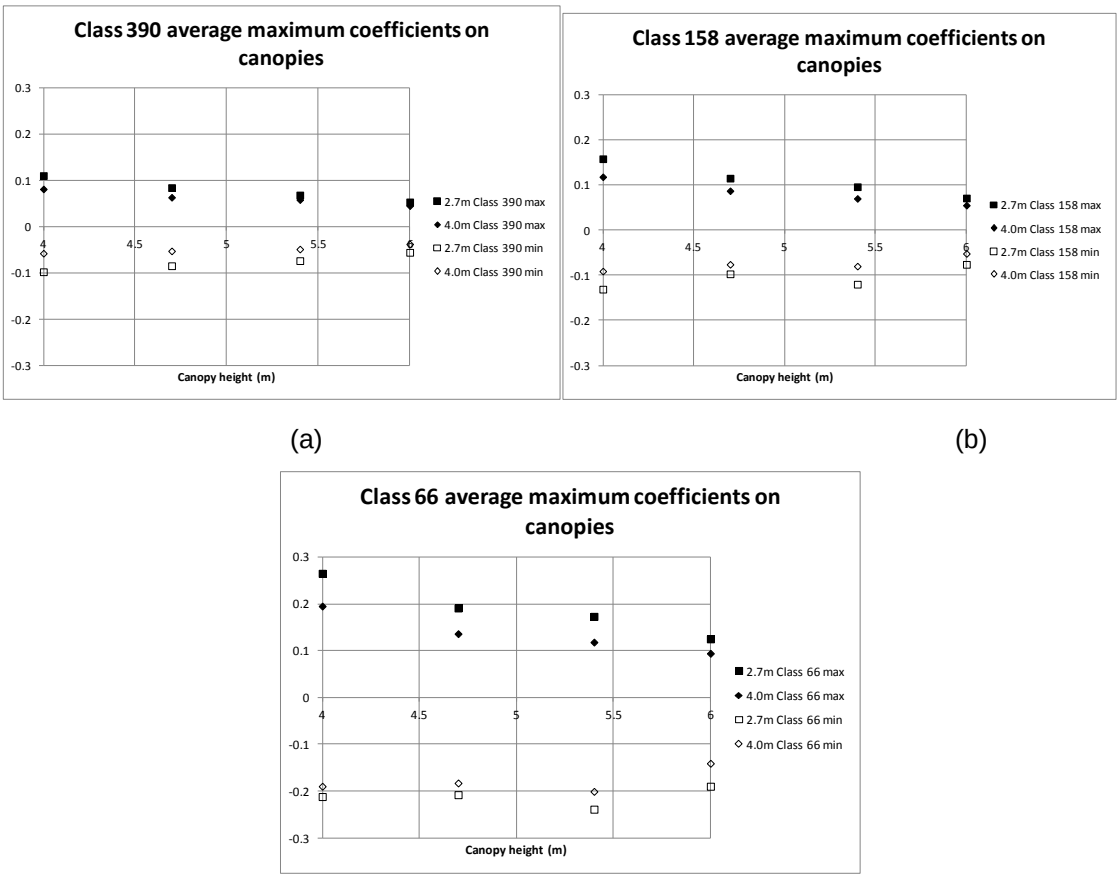


**Figure 9** Maximum pressure coefficients for canopies (numbers in legend indicate back wall distance from nearest rail)

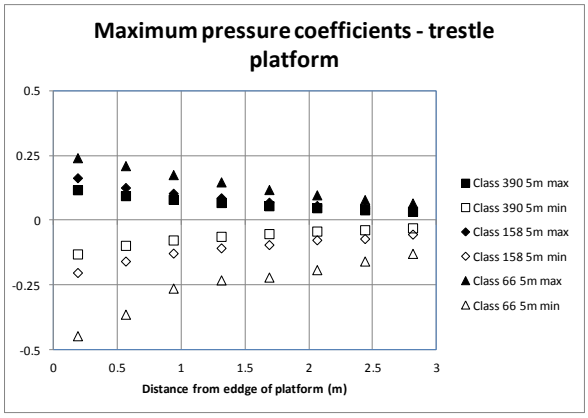


**Figure 10** Maximum pressure coefficient distribution for trestle platform

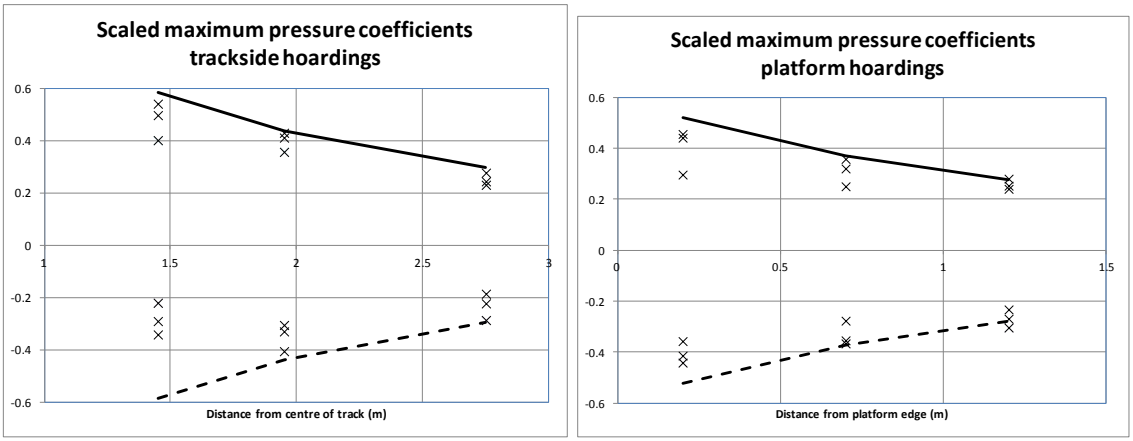


(a) (b)

**Figure 11** Maximum pressure coefficients for hoardings scaled with *k* factors to allow for the effect of different train types. (Vertical axis shows pressure coefficient / *k*; a – trackside hoardings; b – platform hoardings, solid and dotted lines show envelopes to data)

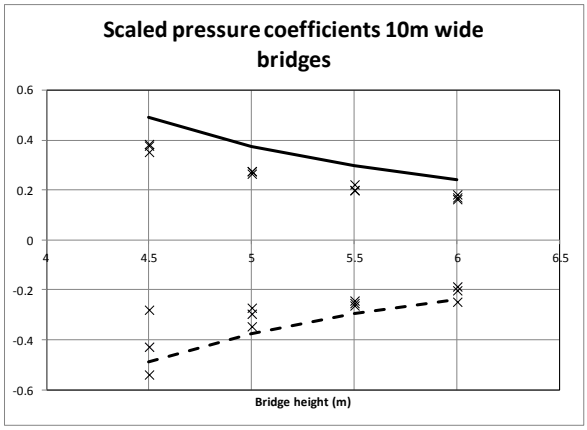


**Figure 12** Maximum pressure coefficients for overbridges scaled with *k* factors to allow for the effect of different train types. (solid and dotted lines show envelopes to data)

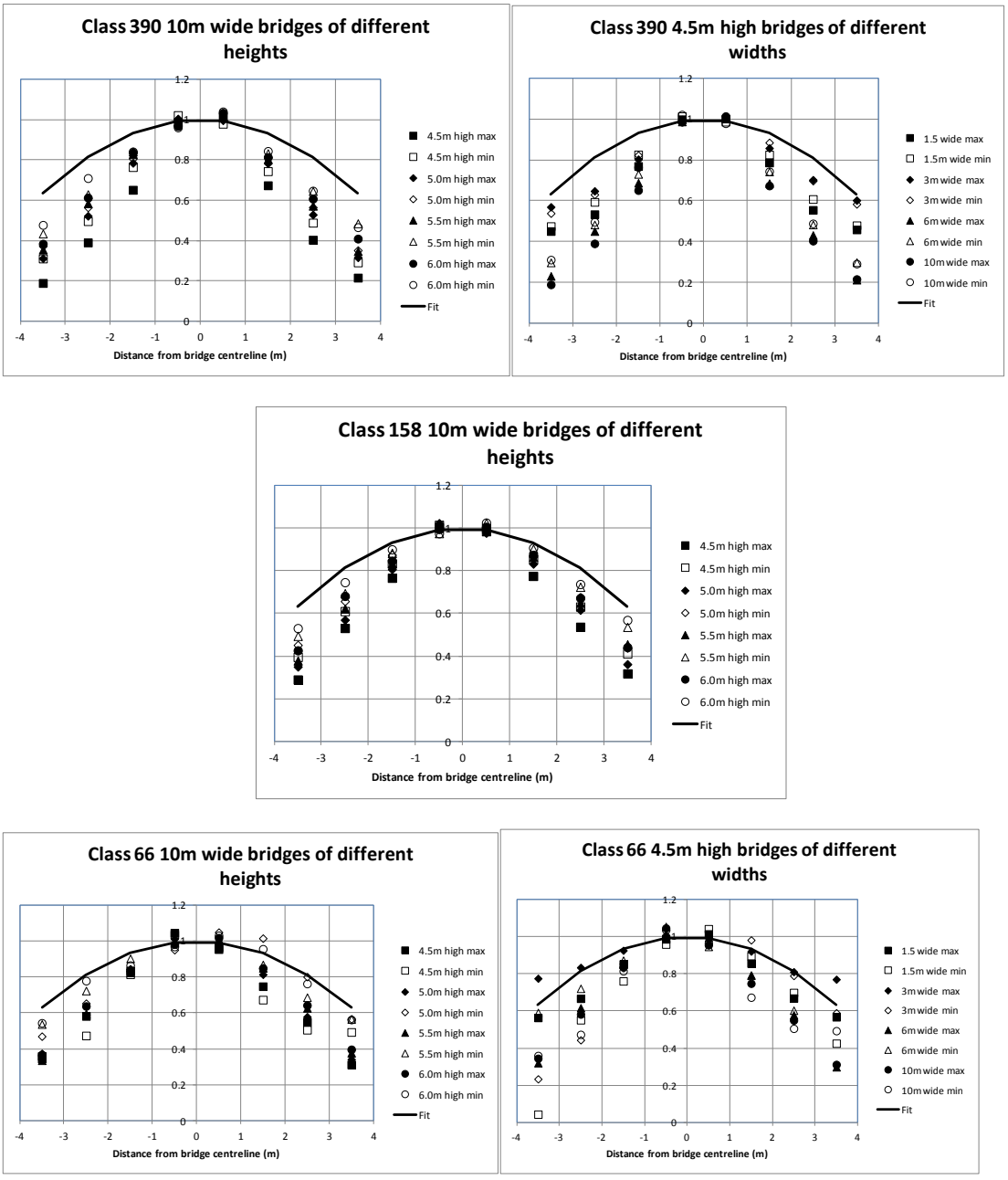


**Figure 13** Lateral variation pressure coefficient ratios for the overbridge results, scaled with centre line values

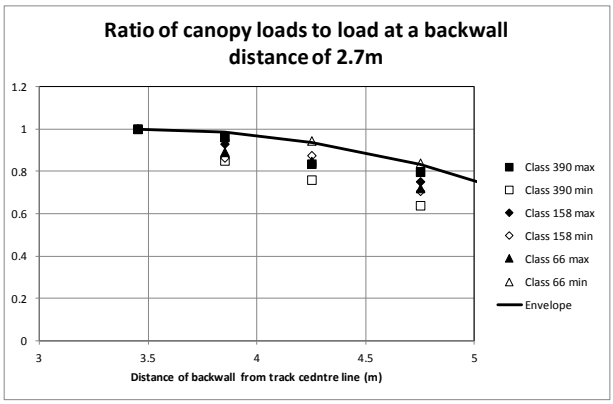


**Figure 14.** Ratio of canopy loads to load with a backwall distance 2.7m from nearest track (3.45m from track centreline) (solid and dotted lines show envelopes to data)

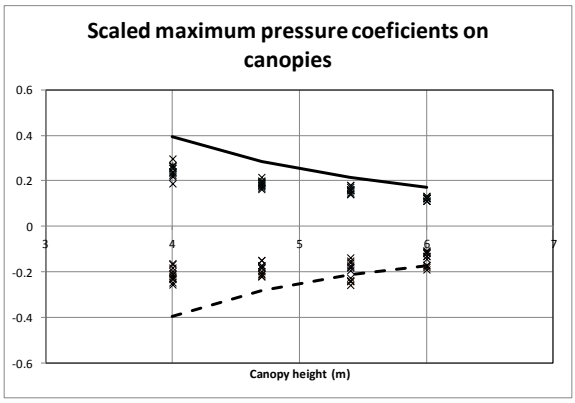


**Figure 15** Canopy experimental pressures divided by *k* and *r* to correct for train type and back wall distance (solid and dotted lines show envelopes to data)

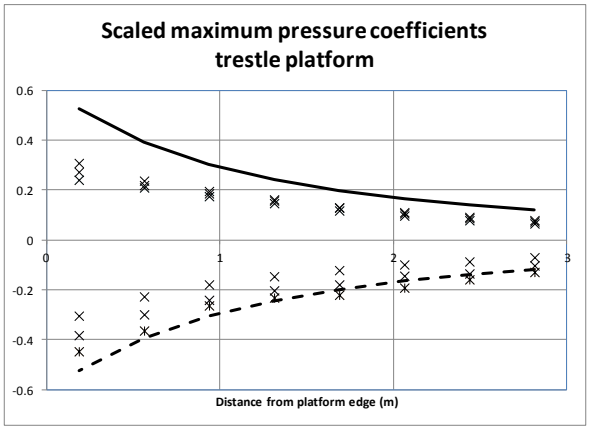


**Figure 16** Experimental pressure coefficients for trestle platform divided by *k* value (solid and dotted lines show envelopes to data **)**

| | Bridge variable height | Bridge variable width | Trestle | Hoarding trackside | Hoarding platform | Canopy 1 | Canopy 2 | Canopy 3 | Canopy 4 | Average values | |
|---|---|---|---|---|---|---|---|---|---|---|---|
| Number of configurations / Weighting in calculating average values | 4 | 4 | 1 | 3 | 3 | 4 | 4 | 4 | 4 | | |
| Class 390 positive peak | 0.421 | 0.409 | 0.473 | 0.494 | 0.547 | 0.417 | 0.45 | 0.412 | 0.462 | 0.447 | 0.426 |
| Class 390 negative peak | 0.535 | 0.707 | 0.256 | 0.357 | 0.402 | 0.368 | 0.323 | 0.291 | 0.277 | 0.404 | |
| Class 158 positive peak | 0.521 | | 0.442 | 0.474 | 0.6 | 0.58 | 0.603 | 0.574 | 0.605 | 0.562 | 0.526 |
| Class 158 negative peak | 0.569 | | 0.442 | 0.474 | 0.6 | 0.496 | 0.448 | 0.461 | 0.415 | 0.489 | |

**Table 1** Ratios of 5m average pres